

Cooperative Flight Control Using Visual-Attention - Air-Guardian

Lianhao Yin¹, Tsun-Hsuan Wang¹, Makram Chahine¹, Tim Seyde¹,
Mathias Lechner¹, Ramin Hasani¹, Daniela Rus¹

Abstract—The cooperation of a human pilot with an autonomous agent during flight control realizes parallel autonomy. A parallel-autonomous system acts as a *guardian* that significantly enhances the robustness and safety of flight operations in challenging circumstances. Here, we propose an air-guardian concept that facilitates cooperation between an artificial pilot agent and a parallel end-to-end neural control system. Our vision-based air-guardian system combines a causal continuous-depth neural network model with a cooperation layer to enable parallel autonomy between a pilot agent and a control system based on perceived differences in their attention profile. The attention profiles are obtained by computing the networks’ saliency maps (feature importance) through the VisualBack-Prop algorithm. The guardian agent is trained via reinforcement learning in a fixed-wing aircraft simulated environment. When the attention profile of the pilot and guardian agents align, the pilot makes control decisions. If the attention map of the pilot and the guardian do not align, the air-guardian makes interventions and takes over the control of the aircraft. We show that our attention-based air-guardian system can balance the trade-off between its level of involvement in the flight and the pilot’s expertise and attention. We demonstrate the effectiveness of our methods in simulated flight scenarios with a fixed-wing aircraft and on a real drone platform.

I. INTRODUCTION

Imagine a pilot navigating an aircraft in low-altitude along a canyon with narrow and wide regions having unpredictable obstacles in its way. The pilot is in full control of navigating the aircraft. This constitutes a challenging flight scenario with high information density, which, depending on the pilot’s level of expertise, can quickly lead to information overload and potentially induce mission-critical failure modes [1]. In this scenario, an intelligent agent that is trained to pilot aircraft autonomously in challenging environments can help to operate in parallel to the pilot with minimal intervention to the human maneuver, enabling air-guardian autonomy.

LY is supported by Knut and Alice Wallenberg Foundation. ML is supported in parts by the ERC-2020-AdG 101020093. This research was partially sponsored by the United States Air Force Research Laboratory and the United States Air Force Artificial Intelligence Accelerator and was accomplished under Cooperative Agreement Number FA8750-19-2-1000. The views and conclusions contained in this document are those of the authors and should not be interpreted as representing the official policies, either expressed or implied, of the United States Air Force or the U.S. Government. The U.S. Government is authorized to reproduce and distribute reprints for Government purposes notwithstanding any copyright notation herein. This work was further supported by The Boeing Company and the Office of Naval Research (ONR) Grant N00014-18-1-2830. The authors thank Paul Tylkin for his contribution to the game environment and their help at the beginning of the project.

¹ Massachusetts Institute of Technology, Computer Science and Artificial Intelligence Laboratory, Cambridge, MA, 02139 USA {lianhao,tsunw, chahine, tseyde, mlechner, rhasani, rus}@mit.edu

Consider the pilot navigating a sharp turn in the canyon with an obstacle suddenly appearing behind the corner. The pilot’s instinct may be to focus attention on immediate obstacle avoidance without considering further stabilizing the turn. This is when the guardian agent can be switched on to safely navigate the airplane with greater precision and attention to both the imminent obstacle and stable flight at the turn. Achieving high levels of autonomy increases the safety of aerial robots in their cooperation with humans and other intelligent agents [2], [3]. An air-guardian system driven by advanced machine learning algorithms can make necessary interventions when a pilot performs poorly. This way, it safely co-pilots the aircraft to its destination, serving as an autopilot system [4]–[6]. The goal of the air-guardian system is to make control decisions based on the actions of the air-guardian and the pilot. The goal is to enable the guardian agent to minimally intervene when the pilot’s decisions and attention may cause an unsafe consequence.

In this paper, we design a novel air-guardian system based on visual attention, which can open new ways through how humans and autonomous agents cooperate. To this end, we first obtain a deep guardian agent via reinforcement learning (RL) in a fixed-wing flight simulator. We additionally design a reference agent (Pilot) by imitation learning or saving early checkpoints of the deep RL guardian agent, which are analogous to artificial pilot agents with different levels of expertise. We then compute the visual attention of both the guardian agent and the imitating pilot agent by computing input importance metrics such as saliency maps. Our air-guardian agent then performs control through a cooperation layer which is a quadratic program that can regulate actions by comparing the attention maps of the two agents, which entails the deviation of decision making. By default, the pilot agent is controlling the aircraft; anytime that the attention profile of the pilot and the guardian agent differs from each other, the guardian agent intervenes, yielding a safer maneuver of the aircraft.

Compared to prior works [7], [8], that make interventions when the control of the pilot is outside of a safety region, our air-guardian system regulates interventions using a visual attention metric. As opposed to other baselines, this cooperation mechanism can potentially identify risky actions much earlier and develop more trust in the human pilot with its inherent interpretability.

Contributions. Our paper makes the following contributions:

1) Introducing a novel cooperative flight control system using visual attention. The cooperative network can assist a human pilot or a robotic pilot who is either less trained to achieve the

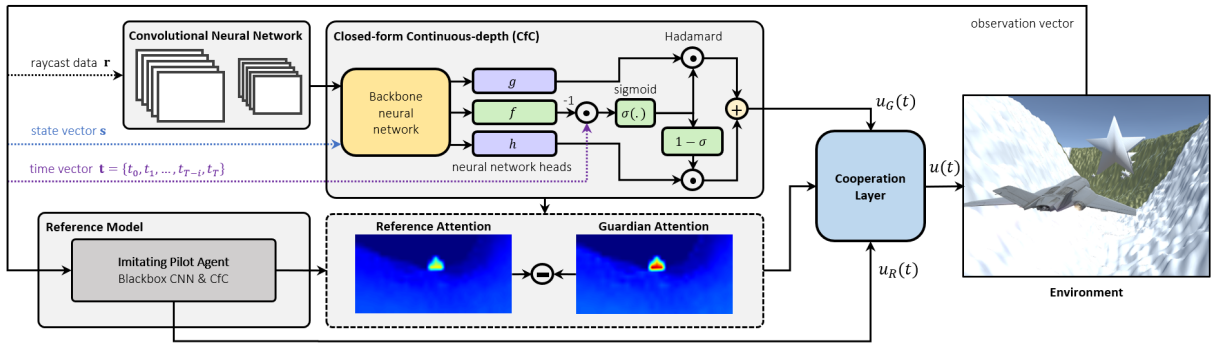


Fig. 1: Cooperative control of pilot and air-guardian. The air-guardian is an autonomous decision system that cooperates with the pilot and the agent to increase the safety of aircrafts. A neural network takes the visual observation from the aircraft and calculates the control input u_G , and the pilot makes a decision and acts with u_R . A cooperative layer decides the real control input u using both u_G and u_R

target or doesn't have certain skills like obstacle avoidance. 2) Integrating a new class of continuous-time neural networks termed the Closed-form Continuous-depth (CfC) models [9] as the guardian to provide robust and causal attention maps. 3) Designing a new cooperative layer via a quadratic program that can switch the control between the guardian and the pilot agent. We deploy the cooperative layer at inference on the trained agent. Nevertheless, in principle, this layer is differentiable and could be trained as well.

II. RELATED WORKS

Human-robot interaction. Human-robotic cooperation is widely used in aerospace [10], vehicle [11], robotic assistant system [12]–[14] and social robots [15]. A few challenges are in human-robotic cooperation are explained here but not limited to these. The goal of the human is unknown to the robotic [13], and one can either predict the goal of the user or formulate the problem as a partially observable Markov decision process. The human in the close-loop with the robot needs to retain trust in the robot [12], the behavior of the robot and human can be mutually adapted to achieve a common goal. People also have different preferences over how much control robots have over them. The end-user could also change the parameter of the closed-loop system and optimize how much control the human possesses [14].

Another way to understand human-robotic cooperation is to consider the cooperation as a safety system, meaning it will make intervention only when reaching critical safety limitations. An intuitive way for humans and robots to cooperate is via a safety system that intervenes in the humans' control commands or provides feedback when a potentially unsafe situation is detected [7]. For example, a car equipped with an assisted-driving system may inform the human driver via haptic feedback when the vehicle leaves the lane [16]. Another approach to combining the control commands of the human and the robot is to assign them a weighting in the form of a linear combination [7], [17].

Air-guardian. An air-guardian describes a system that monitors pilot control commands and switches to automatic control in certain situations [18]. The switching of the control

is triggered by measuring a risk [7] or trust [2] metric. A model based on trust was suggested in [2] to keep track of how frequently errors of the human commands lead to unsafe scenarios. A risk metric of aircraft was proposed in [19] that maps the state of an aircraft and the human's attention to a risk term. The state of the aircraft may comprise the spatial position, aircraft rotation angle, speed, accelerations, and distance to obstacles [20], [21]. For example, a risk metric may evaluate the distance of the aircraft to an obstacle or when the human's attention diverges from the aircraft's destination. The main limitation of such an approach is that the state of an aircraft is not always accurate and available, e.g., distance to obstacles not accessible in visual navigation.

Visual Attention. Saliency maps compute the visual attention of computer vision algorithms that process images, i.e., measuring the importance of the input pixels at inference. Such *attention maps* have been particularly important for analyzing which parts of an image black-box machine learning models focus their attention on [22]–[24]. For example, attention maps have been used to identify the input regions that have the highest influence on the network's output in end-to-end autonomous vehicle control [19], [25]. The eye tracking system is a way to identify the attention of a human [26]. However, this paper is to use the attention profile abstracted from a network that can imitate human behavior instead of eye gazing attention.

Our paper takes advantage of research on attention maps for combining a pilot and a neural network flight controller for autonomous and safe decision-making. Our method shares similarities with the work of [27], which extracts the gaze focus of a human using eye-tracking for action planning. However, our approach can be deployed autonomously without requiring a human operator. This is possible by learning a surrogate human model trained to imitate a human operator.

Safe reinforcement learning. Safety in reinforcement learning has been studied via constrained Markov decision processes (CMDPs) [28]–[30]. CMDPs extend the standard MDPs with auxiliary cost terms provided to the learning and the reward. The objective of CMDPs is then to train a

policy that maximizes the expected total discounted reward while keeping all expected total discounted auxiliary costs below a given threshold. The most common algorithm for solving CMDPs has constrained policy optimization (CPO) [31]. In each training iteration, CPO constructs a trust-region [32] around the current policy known to satisfy the cost constraints and then maximizes the expected total discounted reward within this trust region. Alternatively, reward shaping for standard MDPs has been proposed for incorporating safety specifications into reinforcement learning [33]–[35].

Recurrent neural network. Recurrent neural networks (RNNs) based on ordinary differential equations are known to learn causal relations well [36]. Liquid-time constant network [37], a special type of such differential equations-based RNN, has been shown to be particularly successful at capturing causal dependencies in visual tasks. For example, the attention map of this type of network aligned closer with that of human observers and was more robust to noise perturbations in vehicle and aircraft navigation problems [9], [38]. Moreover, RNNs in general and liquid-time constant networks specifically have been shown to be much more robust to noise than feedforward networks for the same task [38]. For our work, we adopt closed-form continuous-depth models (CfCs) [39], which is a computationally more efficient variant of the liquid-time constant networks [40] that maintain some of its attractive salient learning capabilities, such as expressivity, causality, and robustness.

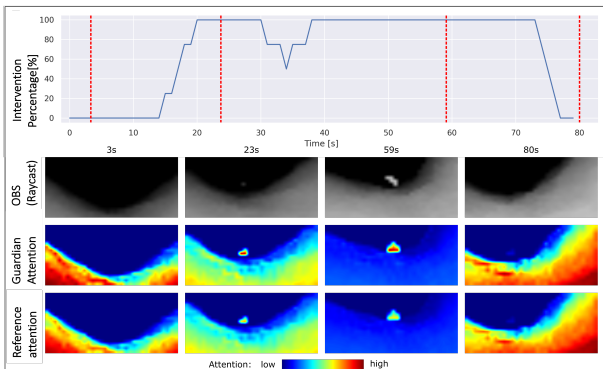


Fig. 2: Comparison of attention profiles and resulting intervention magnitudes over a flight trajectory. The guardian and reference attention map are normalized to give a clear indication of difference.

III. SETUP AND METHODOLOGY

In this section, we introduce our air-guardian concept. Figure 1 shows an overview of our method. The air guardian agent, f_G , is composed of a stack of convolutional layers with closed-form continuous-depth (CfC) recurrent networks. The agent is trained via proximal policy optimization (PPO) [41], a model-free reinforcement learning algorithm in a

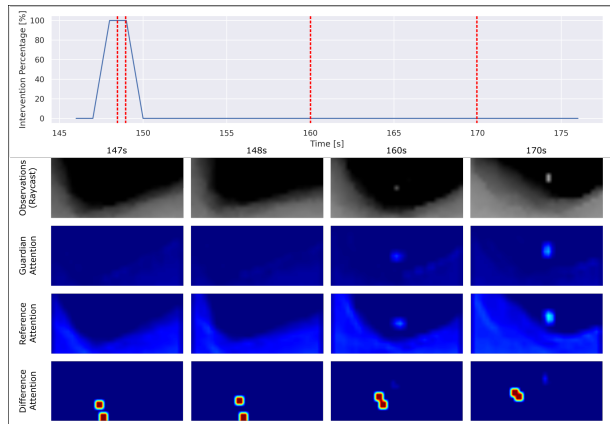


Fig. 3: Comparison of attention profiles and resulting intervention focus over a flight trajectory. The red dots are plotted to indicate the centers of the guardian and reference attention

fixed-wing arcade environment [42]. The reference model f_R can resemble pilots with different levels of expertise.

This imitates the scenario where the pilot suffers from cognitive overload and fails to pay attention to critical environmental information. The goal is to safely navigate the aircraft in a low-altitude canyon environment in the presence of waypoints to be collected and obstacles to be avoided via the cooperation of the guardian and the pilot agent.

The cooperative layer computes the final output u by combining the control input of the guardian network u_G and the reference network input u_R . This is regulated by the difference between the reference attention map and the air-guardian attention map. The difference in reference attention maps can be either the amplitude difference between the two attention maps or the weighted-center distance of the two attention maps. The air-guardian attention map and the reference agent’s attention map are derived by the Visual-BackProp algorithm [24] from the networks f_G and f_R . In the following, we describe each piece in detail.

A. The Guardian agent’s neural model

The air-guardian network takes the incoming images and passes them through convolution layers shown in Fig. 1. The output of the convolution layers is flattened and fed to a dense layer, followed by a CfC network [39]. CfC networks are sequential decision-makers that, with the explicit model of timing behavior and varying time-constant, were shown to capture the underlying causal structure of a given task [39]. This allows the extracted attention map to capture accurate information about the decision making process. The state of the network is calculated by the *liquid* time-gating of g and h (1). Note that the gating is not only determined by the input I , state x , but also by the time t , which makes this network a time-liquid recurrent network [40].

$$\mathbf{z}(t) = \sigma(-f(\mathbf{x}, \mathbf{I}; \theta_f)\mathbf{t}) \odot g(\mathbf{x}, \mathbf{I}; \theta_g) + \quad (1)$$

$$(1 - \sigma(-f(\mathbf{z}, \mathbf{I}; \theta_f)\mathbf{t})) \odot h(\mathbf{x}, \mathbf{I}; \theta_h) \quad (2)$$

The networks of f, g, h share the first few layers as a backbone and then branch out into three functions. The corresponding network parameters are $\theta_f, \theta_g, \theta_h$. The time-decaying sigmoid function σ stands for a gating mechanism that toggles between two continuous trajectories. \odot is the Hadamard (element-wise) product.

B. Visual attention map

The attention maps are calculated by the VisualBackProp algorithm [24]. For a convolutional neural network with weights and bias, we can think of a network flow from images to the output of the network [24]. We denote the activation a_e for one edge e in the particular path P in the general CNN, and \mathcal{P} is a family of path from image to output. From the value of pixel X , denote the backpropagation function [24]: $\phi_f(X) = c\gamma(X) \sum_{P \in \mathcal{P}} \prod_{e \in P} a_e$, where c is the constant and $\gamma(X)$ is the value of pixel. Note that the subscript of the propagation function $\phi_f(X)$ is the network f , upon which the algorithm is used. The saliency maps corresponding to the reference, and guardian networks are $\phi_{f_R}(X)$ and $\phi_{f_G}(X)$.

C. Cooperative network

The cooperative network computes the final control u by optimizing the pilot control u_R and the air-guardian's u_G , taking into account the difference of the attention map of the pilot agent $\phi_{f_R}(X)$ and the guardian's $\phi_{f_G}(X)$. Let us denote the weighted centers of air-guardian saliency map and pilot saliency map as $d_{\phi_{f_R}}$ and $d_{\phi_{f_G}}$, respectively. Denote the aircraft system as $\mathbf{x}_{k+1} = g(\mathbf{x}_k, u)$ with input u , state \mathbf{x} and output $\mathbf{y}_k = q(\mathbf{x}_k)$. A safety set is defined as \mathbb{S} . Moreover, let I be the intervention of the guardian agent in the flight operation. The air-guardian will take control if $I = 1$ while the pilot agent will take control if $I = 0$. The switching of I is regulated by either the amplitude difference (Eq. 3) or the weighted-center distance of the attention maps (Eq. 4).

$$I = \begin{cases} 1 & \|\phi_{f_R} - \phi_{f_G}\| \leq c_f \\ 0 & \|\phi_{f_R} - \phi_{f_G}\| > c_f \end{cases} \quad I = \begin{cases} 1 & \|d_{\phi_{f_R}} - d_{\phi_{f_G}}\| \leq d_f \\ 0 & \|d_{\phi_{f_R}} - d_{\phi_{f_G}}\| > d_f \end{cases} \quad (3) \quad (4)$$

where c_f and d_f are the thresholds of the amplitude difference and weighted-center distance, respectively.

The optimization problem minimizes the difference in the control outputs of the reference and air-guardian as follows:

$$\begin{aligned} \min_{\mathbf{u}_{k+1, k+2, \dots, k+H_p}} & \sum_{i=k}^{i=k+H_p} \|\mathbf{u}_i - \mathbf{u}_{R_i}\|_{Q_h} + I \|\mathbf{u}_i - \mathbf{u}_{G_i}\|_{Q_G} \\ \text{s.t.} & \quad \mathbf{x}_{k+1} = g(\mathbf{x}_k, u_k) \\ & \quad \mathbf{y}_k = q(\mathbf{x}_k) \\ & \quad \mathbf{y}_k \in \mathbb{S}, \end{aligned} \quad (5)$$

where H_p is the prediction horizon. The solution of the optimization keeps the final control output u close to the u_R when there is a small deviation in the attention profile of the reference and air-guardian agent. While the solution keeps the final control u close to u_G when there is a large deviation. The optimization problem Eq. 5 is differentiable

and can be a layer of a neural network [43]. This cooperation layer concludes our air-guardian concept. In the next section, we first discuss the robustness properties of the cooperative layer. We then describe our experimental setting and results.

IV. EXPERIMENTAL RESULTS IN SIMULATION

The experimental platform is an environment chosen from the autonomous flight arcade proposed in [42]. The aircraft is a fixed-wing with the ability to roll, pitch, yaw, and throttle. The basic aerodynamic effects are modeled. However, it does not consider the turbulence between the aircraft and its nearby objects. The observations are raycasting which can be considered as Lidar signals. Therefore the sim-2-real gap can be minimized. The reward comes from collecting waypoints, which are represented as stars in the scene. One gains a reward at each catch of a waypoint.

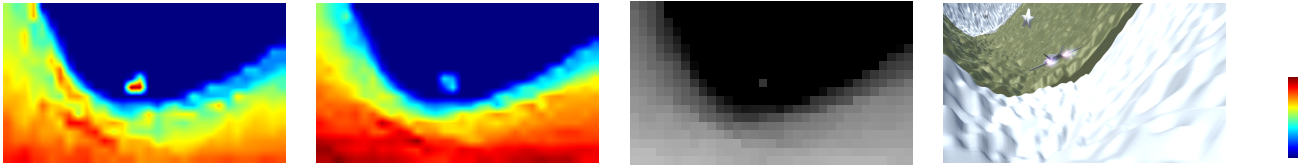
A. Training setup

The neural networks (f_G and f_R defined in Sec. III) were trained using a model-free RL algorithm, Proximal Policy Optimization (PPO) [41]. PPO was implemented in RLLib [44]. The air-guardian policy f_G shown in Figure 1 was obtained by PPO to obtain maximum rewards by navigating along the canyon environment in experiment 1 and was trained by PPO to maximize the reward of surviving in experiment 2. The reference network f_R is obtained by earlier checkpoints (with 80 % performance of a well-trained agent) of the PPO policy for simulated pilot one and is obtained by training with different reward functions for simulated pilot 2.

The guardian can both assist (1) a less proficient agent, which was represented as a network with an earlier checkpoint, and (2) an agent without certain skills such as obstacle avoidance. Two experiments were used to verify the guardian concept. In the first experiments, both reference (Simulated pilot 1) and guardian network were trained to catch as many waypoints as possible while avoiding dynamic obstacles. The intervention profile for the guardian is the attention amplitude. The first experiment uses the simulated pilot one as a less proficient agent. In the second experiment, the reference (simulated pilot 2) is trained without obstacles, and the guardian is trained only to avoid obstacles yet not to catch waypoints, which resembles a safety-focused decision-maker. The intervention profile for the guardian is the weighted center distance of the pilot and guardian attention maps. The weighted center is defined as $d_c = \sum w_i x / \sum w_i$, where the w_i is the weight of each pixel and x is the position of each pixel. The weighted-center distance is the center distance of two attention maps ($|d_{c_1} - d_{c_2}|$). The second experiment uses the reference network to represent an artificial pilot who has a less proficient skill in obstacle avoidance.

B. Results: guardian intervention

In the first experiments, the intervention process using control policy from (3) and (5) is illustrated in Fig. 2. When the control is fully regulated by u_G , the intervention level is at 100 %, and when the control is computed by



(a) Attention map using CfC network.

(b) Attention map using LSTM.

(c) Ray cast images from the observation

(d) Game image of current situation

Fig. 4: Comparison of attention maps (computed by VisualBackProp) between CfC and LSTM. The small dot is light blue and less visible and distinguishable from the rest of the figure (Fig. 4b). The small red dot is visible and distinguishable from the rest of the figure (Fig. 4a).

u_R , the intervention level is at 0 %. When there is no guardian intervention at 3s in Fig. 2, the attention maps of air-guardian Fig. 2 have a quite similar level to that of the reference network Fig. 2. When the intervention level reaches 100 % at 23s in Fig. 2, the intensity of the attention on waypoint Fig. 2 on the attention map of the air-guardian network is much stronger than that of the reference network Fig. 2. It is intuitive to understand that the air-guardian makes interventions when the aircraft is approaching the waypoint. This is true for the case where the reference agent (pilot) is not as good at catching the waypoints as the guardian agent.

In the second experiments, the intervention process using control policy from (4) and (5) is illustrated in Fig. 3. Similar to the first experiment, the control is fully regulated by u_G when the intervention is at 100 % and fully regulated by u_R when the intervention level is at 0 %. The control policy from (4) has a more cognitive motivation that when the difference of the attention focuses exceeds a threshold, the guardian takes intervention. Intuitively, when the attention of the pilot focuses on a wrong place, the guardian will take control. This is especially important when pilots do not pay attention to the safety critical point in vision due to highly dense information from other aircraft operations. This resembles the cognitive overload situation, which is often one of the major factors of accidents in real-world aviation.

C. Results: cooperative control performance

In the first experiment, the intervention used amplitude difference of guardian and reference attention maps (3). The pilot is not well trained to achieve the designed task (Catching the waypoint and avoiding obstacles). We observe that the pilot prefers to catch as many waypoints as possible to obtain more rewards. The results show that the air-guardian can improve the performance of the pilot, as illustrated in Tab. I. We compared it with another cooperative mechanism called shielding [8]. We construct a shielding control based on the L2 norm of the difference between the control of the reference and the air-guardian agents. If the difference of control is outside a *shield*, the air-guardian will intervene and take control of the aircraft. The baseline uses a network to imitate human performance. The tests were conducted in the Canyon-run environment [42]. The results (Tab. II) show that our proposed attention-based cooperative control can improve 13% of performance above the simulated-reference pilot and considerably outperforms the shielding method.

Name	Mean	std
Pilot 1	9.2	0.37
guardian	10.5	0.66
Shield	8.1	0.64

TABLE I: Results. Experiment 1: P1: Simulated pilot 1 (not well trained). G(P1): Air-guardian with P1. S(P1): shield with P1.

Name	Mean (P2)	Mean(GP2)	std(P2)	std(GP2)
Risk level(%)	86	0	35	0

TABLE II: Results. Experiment 2: P2: Simulated pilot 2(No certain skills such as obstacle avoidance). G(P2): Air-guardian with P2. Each experiment conducted multiple runs, 15 each

In the second experiment, the intervention criteria used weighted-center-distance of guardian and pilot attention maps. The guardian can assist an artificial pilot who has no certain skills. Pilot 2 was trained without obstacles and only rewarded by catching a waypoint, and the guardian was trained only to avoid obstacles. The intervention policy defined in (4) can supplement skills to the reference network(P2 in Tab. I and Tab. II) and improves its performance in obstacle avoidance. In the second experiment shown in Tab. II), We compared the collision rate using the guardian and without using the guardian. We observed that the collision rate of the reference pilot is 86% and the collision rate with guardian 0 % over a constant length of flights with a p-value ($3.7e^{-7} < 0.05$). The difference is significant.

D. Analysis: robustness of the visual attention maps

To justify the choice of the CfC model in our framework, we performed an additional experiment comparing the attention profile of a long short-term memory (LSTM) [45] with that of a CfC network. We train both modules with the same PPO algorithm. They both accumulate the same amount of rewards. For this experiment, the attention profiles are given in Fig. 4. When the aircraft approaches the waypoint, the focus on the waypoint in the attention map generated from CfC (Fig. 4a) is much more evident than that of LSTM (Fig. 4b). This enhances the robustness of the guardian agent as our concept is dependent on the attention profile of the pilot and guardian agent.

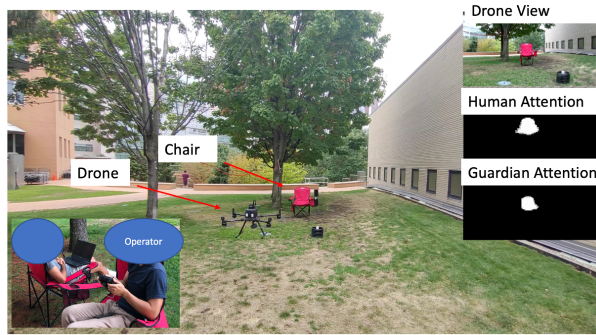


Fig. 5: The experiment consists of having a human pilot a quadrotor towards a target. Three subviews are drone’s view, human attention and guardian attention

Name	Mean (P)	Mean(GP)	std(P)	std(GP)	p value
$max(d)$	1.03	0.86	0.55	0.62	0.05
$max(v)$	1.56	1.10	0.52	0.50	1.57×10^{-6}

TABLE III: The speed of the drone in a different direction is used to evaluate the performance of the human pilot (P) and human pilot with a guardian (GP). The maximum drone speed $max(v)$ with a guardian is smaller than that of without a guardian. The maximum distance between the flying trace and optimal flying trace is defined as $max(d)$. The $max(d)$ with guardian is shorter than that without guardian.

E. Analysis: interpretability

The attention map provides an intuitive representation of the key features the agent focuses on during its decision-making process since it highlights the saliency of key features in the environment. This makes potential mismatches in attention profiles and resulting interventions readily interpretable. Specifically, the part of the attention map with a higher value has a stronger influence on the output action. The attention intensity of the waypoint in the air-guardian’s attention map is very strong at 23 seconds (Fig. 2, second frame middle row, dark red). In contrast, the reference agent’s attention is primarily focused on the canyon walls, and the attention attributed to the waypoint is significantly reduced at 23 seconds (Fig. 2, second frame bottom row, light blue). It is straightforward to interpret the difference in the attention maps of the guardian and reference agent based on mismatches in highlighted key environment features. When the difference of attention map exceeds the threshold given in (3) or (4), the air-guardian intervenes to take dominant control of the aircraft. From a causal reasoning perspective, the reference agent has a lower performance to achieve a high reward in the designed mission and bases its decision primarily on environmental constraints. The guardian agent is able to negotiate a trade-off between safety and mission completion by distributing attention among the environment constraints and waypoint objectives.

V. HUMAN-IN-THE-LOOP RESULTS ON A REAL DRONE

We test our cooperative control structure (Fig. 1) presented in Sec. III on a quadrotor platform; a DJI M300 RTK.

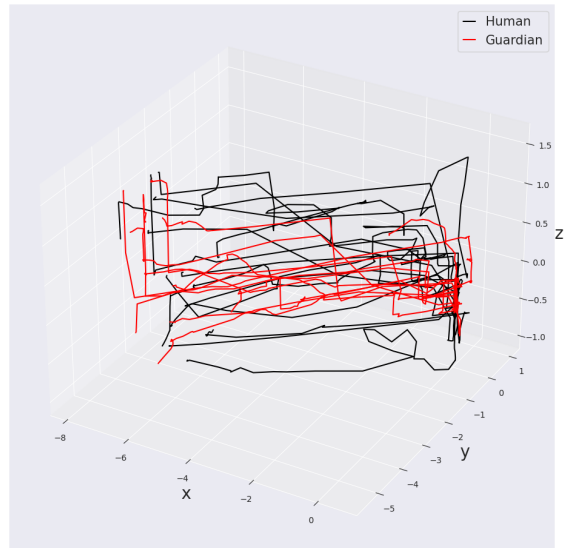


Fig. 6: Flying trajectory of human and guardian. The origin on the right side of the image is the target and the drone start from the left side

The quadcopter has an onboard computer companion (DJI Manifold 2) that enables programmatic control of the drone. Input images are gathered from a Zenmuse Z30 camera stabilized on a gimbal. The experiment consists of having a human pilot the quadrotor towards a target (red camping chair) with/without the help of the attention map-based guardian (Fig. 5). In total, six people have been in the experiments and each person have repeat the task 16 times with four different starting points. Among the 16 flights, 8 are performed solely by the human and the other 8 performed with the guardian system on (Fig. 6).

The pretrained CfC architecture is used for the guardian as f_G defined in Sec. III, while a Gated recurrent unit - Ordinary Differential Equation (GRU-ODE) network as f_R defined in Sec. III is used to represent the human pilot’s attention map. Both networks were pretrained on sequences of images of expert task demonstrations using a Behavior-Cloning (BC) Mean Squared Error (MSE) loss. The intervention criterion is the distance between the weighted center of human and guardian attention as per (4). The threshold value is manually calibrated such that intervention occurs when the drone is flying away from the target, and the target is almost outside the drone’s view.

The results (Tab. III) have shown that the guardian system can help fly the drone to reach the target with a lower flight speed and shorter distance to the optimal flying-trajectory, meaning a smaller risk of hitting other obstacles. The p-value is less than 0.05, and the difference is significant.

VI. CONCLUSION

We proposed a visual-attention-based air-guardian concept and showed that the proposed method could improve the

performance of a simulated pilot in the task of capturing waypoints by cooperation. The air-guardian system makes causal interventions based on the attention difference between the air-guardian and simulated pilot. The performance of the simulated pilot is improved when the air-guardian is in place. Our results demonstrate that the proposed cooperative flight control can balance the trade-off between the level of involvement in the flight and the pilots' expertise in the simulated flight scenarios.

REFERENCES

- [1] M. A. J. T. DeVeans, L. T. C. R. H. Kewley, and P. D., "Overcoming Information Overload in the Cockpit Sponsored by Program Executive Office - Soldier," *Operations Research*, no. July, 2009.
- [2] J. Lee and N. Moray, "Trust, control strategies and allocation of function in human-machine systems," *Ergonomics*, vol. 35, no. 10, pp. 1243–1270, 1992.
- [3] D. Sofge, W. Lawless, and R. Mittu, "Ai bookie: Will a self-authorizing ai-based system take control from a human operator?" *AI Magazine*, vol. 40, no. 3, pp. 79–84, 2019.
- [4] H. Chao, Y. Cao, and Y. Q. Chen, "Autopilots for small fixed-wing unmanned air vehicles: A survey," *Proceedings of the 2007 IEEE International Conference on Mechatronics and Automation, ICMA 2007*, pp. 3144–3149, 2007.
- [5] M. Dikmen and C. Burns, "Trust in autonomous vehicles: The case of tesla autopilot and summon," in *2017 IEEE International Conference on Systems, Man, and Cybernetics (SMC)*, 2017, pp. 1093–1098.
- [6] J. Jackson, D. Koch, T. Henrichsen, and T. McLain, "ROSflight: A lean open-source research autopilot," *IEEE International Conference on Intelligent Robots and Systems*, pp. 1173–1179, 2020.
- [7] W. Schwarting, J. Alonso-Mora, and D. Rus, "Planning and Decision-Making for Autonomous Vehicles," *Annual Review of Control, Robotics, and Autonomous Systems*, vol. 1, pp. 187–210, 2018.
- [8] M. Alshiekh, R. Bloem, R. Ehlers, B. Könighofer, S. Niekum, and U. Topcu, "Safe reinforcement learning via shielding," *32nd AAAI Conference on Artificial Intelligence, AAAI 2018*, pp. 2669–2678, 2018.
- [9] C. Vorbach, R. Hasani, A. Amini, M. Lechner, and D. Rus, "Causal navigation by continuous-time neural networks," *Advances in Neural Information Processing Systems*, vol. 34, pp. 12425–12440, 2021.
- [10] H. Zhu, R. Xu, and M. L. Cummings, "Quantitative operator strategy comparisons across human supervisory control scenarios," *IEEE International Conference on Intelligent Robots and Systems*, pp. 10968–10974, 2020.
- [11] W. Schwarting, J. Alonso-Mora, L. Pauli, S. Karaman, and D. Rus, "Parallel autonomy in automated vehicles: Safe motion generation with minimal intervention," *Proceedings - IEEE International Conference on Robotics and Automation*, pp. 1928–1935, 2017.
- [12] S. Nikolaidis, Y. X. Zhu, D. Hsu, and S. Srinivasa, "Human-Robot Mutual Adaptation in Shared Autonomy," *ACM/IEEE International Conference on Human-Robot Interaction*, vol. Part F127194, pp. 294–302, 2017.
- [13] S. Javdani, S. S. Srinivasa, and J. A. Bagnell, "Shared autonomy via hindsight optimization," *Robotics: Science and Systems*, vol. 11, 2015.
- [14] D. Gopinath, S. Jain, and B. D. Argall, "Human-in-the-loop optimization of shared autonomy in assistive robotics," *IEEE Robotics and Automation Letters*, vol. 2, no. 1, pp. 247–254, 2017.
- [15] M. Carvalho, J. Avelino, A. Bernardino, R. Ventura, and P. Moreno, "Human-Robot greeting: tracking human greeting mental states and acting accordingly," *2021 IEEE/RSJ International Conference on Intelligent Robots and Systems (IROS)*, no. i, pp. 1935–1941, 2021.
- [16] D. A. Abbink, M. Mulder, and E. R. Boer, "Haptic shared control: Smoothly shifting control authority?" *Cognition, Technology and Work*, vol. 14, no. 1, pp. 19–28, 2012.
- [17] S. J. Anderson, S. B. Karumanchi, K. Iagnemma, and J. M. Walker, "The intelligent copilot: A constraint-based approach to shared-adaptive control of ground vehicles," *IEEE Intelligent Transportation Systems Magazine*, vol. 5, no. 2, pp. 45–54, 2013.
- [18] A. W. Knapp, "AirGuardian : A Parallel Autonomy Approach to Self-Flying Planes by," Master's thesis, Massachusetts Institute of Technology, 2020.
- [19] J. Kim and J. Canny, "Interpretable Learning for Self-Driving Cars by Visualizing Causal Attention," *Proceedings of the IEEE International Conference on Computer Vision*, vol. 2017-October, pp. 2961–2969, 2017.
- [20] N. Wessendorp, R. Dinaux, J. Dupeyroux, and G. C. H. E. de Croon, "Obstacle Avoidance onboard MAVs using a FMCW Radar," *2017 IEEE International Conference on Computer Vision (ICCV)*, pp. 117–122, 2021.
- [21] S. Xu, D. Honegger, M. Pollefeys, and L. Heng, "Real-time 3D navigation for autonomous vision-guided MAVs," *IEEE International Conference on Intelligent Robots and Systems*, vol. 2015-December, pp. 53–59, 2015.
- [22] Y. Lecun, Y. Bengio, and G. Hinton, "Deep learning," *Nature*, vol. 521, no. 7553, pp. 436–444, 2015.
- [23] K. Xu, J. L. Ba, R. Kiros, K. Cho, A. Courville, R. Salakhutdinov, R. S. Zemel, and Y. Bengio, "Show, attend and tell: Neural image caption generation with visual attention," *32nd International Conference on Machine Learning, ICML 2015*, vol. 3, pp. 2048–2057, 2015.
- [24] M. Bojarski, A. Choromanska, K. Choromanski, B. Firner, L. Jackel, U. Muller, and K. Zieba, "VisualBackProp: efficient visualization of CNNs," 2016. [Online]. Available: <http://arxiv.org/abs/1611.05418>
- [25] S. Yang, W. Wang, C. Liu, and W. Deng, "Scene understanding in deep learning-based end-to-end controllers for autonomous vehicles," *IEEE Transactions on Systems, Man, and Cybernetics: Systems*, vol. 49, no. 1, pp. 53–63, 2019.
- [26] R. M. Aronson, T. Santini, T. C. Kübler, E. Kasneci, S. Srinivasa, and H. Admoni, "Eye-Hand Behavior in Human-Robot Shared Manipulation," *ACM/IEEE International Conference on Human-Robot Interaction*, pp. 4–13, 2018.
- [27] L. Paletta, M. Pszeida, H. Ganster, F. Fuhrmann, W. Weiss, S. Ladstatter, A. Dini, S. Murg, H. Mayer, I. Brijacak, and B. Reiterer, "Gaze-based Human Factors Measurements for the Evaluation of Intuitive Human-Robot Collaboration in Real-time," *IEEE International Conference on Emerging Technologies and Factory Automation, ETFA*, vol. 2019-September, no. L, pp. 1528–1531, 2019.
- [28] E. Altman, *Constrained Markov decision processes*. CRC Press, 1999, vol. 7.
- [29] P. Geibel, "Reinforcement learning for mdps with constraints," in *Machine Learning: ECML 2006, 17th European Conference on Machine Learning, Berlin, Germany, September 18-22, 2006, Proceedings*, ser. Lecture Notes in Computer Science, J. Fürnkranz, T. Scheffer, and M. Spiliopoulou, Eds., vol. 4212. Springer, 2006, pp. 646–653. [Online]. Available: https://doi.org/10.1007/11871842_63
- [30] E. Uchibe and K. Doya, "Constrained reinforcement learning from intrinsic and extrinsic rewards," in *2007 IEEE 6th International Conference on Development and Learning*. IEEE, 2007, pp. 163–168.
- [31] J. Achiam, D. Held, A. Tamar, and P. Abbeel, "Constrained policy optimization," in *International Conference on Machine Learning. PMLR*, 2017, pp. 22–31.
- [32] J. Schulman, S. Levine, P. Abbeel, M. Jordan, and P. Moritz, "Trust region policy optimization," in *International conference on machine learning*. PMLR, 2015, pp. 1889–1897.
- [33] A. Ray, J. Achiam, and D. Amodei, "Benchmarking safe exploration in deep reinforcement learning," *arXiv preprint arXiv:1910.01708*, vol. 7, p. 1, 2019.
- [34] K. Jothimurugan, R. Alur, and O. Bastani, "A composable specification language for reinforcement learning tasks," *Advances in Neural Information Processing Systems*, vol. 32, 2019.
- [35] Y. Jiang, S. Bharadwaj, B. Wu, R. Shah, U. Topcu, and P. Stone, "Temporal-logic-based reward shaping for continuing reinforcement learning tasks," in *Proceedings of the AAAI Conference on Artificial Intelligence*, vol. 35, no. 9, 2021, pp. 7995–8003.
- [36] B. Schölkopf, "Causality for machine learning," *arXiv preprint arXiv:1911.10500*, 2019.
- [37] R. Hasani, M. Lechner, A. Amini, D. Rus, and R. Grosu, "Liquid Time-constant Networks," 2020. [Online]. Available: <http://arxiv.org/abs/2006.04439>
- [38] M. Lechner, R. Hasani, A. Amini, T. A. Henzinger, D. Rus, and R. Grosu, "Neural circuit policies enabling auditable autonomy," *Nature Machine Intelligence*, vol. 2, no. 10, pp. 642–652, 2020. [Online]. Available: <http://dx.doi.org/10.1038/s42256-020-00237-3>
- [39] R. Hasani, M. Lechner, A. Amini, L. Liebenwein, M. Tschaikowski, G. Teschl, and D. Rus, "Closed-form continuous-depth models," *arXiv preprint arXiv:2106.13898*, 2021.

- [40] R. Hasani, M. Lechner, A. Amini, D. Rus, and R. Grosu, "Liquid time-constant networks," in *Proceedings of the AAAI Conference on Artificial Intelligence*, vol. 35, 9, 2021, pp. 7657–7666.
- [41] J. Schulman, F. Wolski, P. Dhariwal, A. Radford, and O. Klimov, "Proximal Policy Optimization Algorithms," pp. 1–12, 2017. [Online]. Available: <http://arxiv.org/abs/1707.06347>
- [42] P. Tylkin, T.-H. Wang, T. Seyde, K. Palko, R. Allen, D. Rus, and A. Amini, "Autonomous Flight Arcade Challenge: Single- and Multi-Agent Learning Environments for Aerial Vehicles," in *International Conference on Autonomous Agents and Multiagent Systems*, Auckland, US, 2022.
- [43] B. Amos and J. Z. Kolter, "OptNet: Differentiable optimization as a layer in neural networks," in *Proceedings of the 34th International Conference on Machine Learning*, ser. Proceedings of Machine Learning Research, vol. 70. PMLR, 2017, pp. 136–145.
- [44] E. Liang, R. Liaw, P. Moritz, R. Nishihara, R. Fox, K. Goldberg, J. E. Gonzalez, M. I. Jordan, and I. Stoica, "RLlib: Abstractions for distributed reinforcement learning," *35th International Conference on Machine Learning, ICML 2018*, vol. 7, pp. 4768–4780, 2018.
- [45] S. Hochreiter and J. Schmidhuber, "Long Short-Term Memory," *Neural Computation*, vol. 9, no. 8, pp. 1735–1780, 11 1997. [Online]. Available: <https://doi.org/10.1162/neco.1997.9.8.1735>